25. E. V. Chulkov, I. Sarria, V. M. Silkin, J. M. Pitarke, P. M. Echenique, *Phys. Rev. Lett.* **80**, 4947 (1998).
26. E. V. Chulkov, V. M. Silkin, P. M. Echenique, *Surf. Sci.* **437**, 330 (1999).
27. E. D. Palik, *Handbook of Optical Constants of Solids* (Academic Press, Boston, 1985).
28. The same approach to *d*-screening applied to bulk line widths reduces them by a factor of $\varepsilon = 2.4$ for Cu. A recent first-principles calculation has shown that *d*-electrons decrease the line width of bulk states in Cu by a factor of 2.4, in excellent agreement with this model (*33*).
29. L. Bürgi, O. Jeandupeux, H. Brune, K. Kern, *Phys. Rev. Lett.* **82**, 4516 (1999).
30. S. LaShell, B. A. McDougall, E. Jensen, *Phys. Rev. Lett.* **77**, 3419 (1996).
31. W. Chen, V. Madhavan, T. Jamneala, M. F. Crommie, *Phys. Rev. Lett.* **80**, 1469 (1998).
32. V. N. Kostur and B. Mitrovic, *Phys. Rev. B* **48**, 16388 (1993).
33. I. Campillo, J. M. Pitarke, A. Rubio, E. Zarate, P. M. Echenique, *Phys. Rev. Lett.* **83**, 2230 (1999).

34. J.K. and R.B. thank the Deutsche Forschungsgemeinschaft for support via Sonderforschungsbereich 341. S.C. acknowledges the support of the Engineering and Physical Sciences Research Council. P.M.E. acknowledges the Max Planck Research Award funds. We thank N. Lorente for discussions.

31 January 2000; accepted 5 April 2000

Real-Time Observation of Adsorbate Atom Motion Above a Metal Surface

Hrvoje Petek,*†‡ Miles J. Weida, Hisashi Nagano, Susumu Ogawa

The dynamics of cesium atom motion above the copper(111) surface following electronic excitation with light was studied with femtosecond (10^{-15} seconds) time resolution. Unusual changes in the surface electronic structure within 160 femtoseconds after excitation, observed by time-resolved two-photon photoemission spectroscopy, are attributed to atomic motion in a copper–cesium bond-breaking process. Describing the change in energy of the cesium antibonding state with a simple classical model provides information on the mechanical forces acting on cesium atoms that are "turned on" by photoexcitation. Within 160 femtoseconds, the copper–cesium bond extends by 0.35 angstrom from its equilibrium value.

The observation of atomic and molecular dynamics on surfaces is a long-standing goal in surface science (*1–3*). Traditional measurements of the energy and momentum deposited in the gas-phase products provide only indirect information on surface processes (*4, 5*). However, time-resolved spectroscopies using femtosecond-duration laser pulses have finally allowed direct observation of surface dynamics in real time (*6*). For example, elegant time-resolved photoemission experiments on image potential states have charted coherent surface electron motion and electron trapping and localization by adsorbates (*7, 8*). Strong excitation-induced coupling between the electrons and nuclei also occurs on a femtosecond time scale; however, to date there has been no equivalent observation of nuclear dynamics on surfaces. The recent discovery of an unusually long-lived electronic state for Cs on Cu(111) (*9*) makes it possible to record the nuclear motion upon electronic excitation. Here, time-resolved photoemission spectroscopy is used to take a "movie" (13.4 fs per frame) of the change in Cs/Cu surface electronic structure in the process of breaking the Cu–Cs bond. Inverting this electronic response reveals the real-time dissociative motion of an atom on a surface.

A logical starting point for discussing the photodesorption dynamics is the potential energy surfaces (PESs) for Cs on Cu (Fig. 1A). Despite the fundamental importance of alkali atom chemisorption in catalysis and thermionic emission, only selected aspects of the ground- and excited-state PESs along the Cu–Cs internuclear coordinate ($R_{\text{Cu-Cs}}$) are known (*10, 11*). The electronic character of the two lowest lying states can be understood from simple atomic orbital ideas. Near a metal, the highest occupied and lowest unoccupied electron orbitals of highly polarizable Cs atoms combine to form a $6s$–$6p_z$ bonding and $6s+6p_z$ antibonding pair in which the electron density is concentrated at the surface or vacuum side, respectively, of the Cs atom (*12, 13*). Optical coupling of the ground- and excited-state PESs induces significant charge redistribution about the alkali atom, considerably weakening the Cu–Cs bond (*14*). Because photoexcitation is much faster than nuclear motion, it projects the ground-state Cs atom probability distribution (wave packet) onto the repulsive wall of the excited state. The ensuing wave packet motion corresponds to the Menzel-Gomer-Redhead scenario for photodesorption (*1, 2*).

The wave packet evolution can be observed because the $6s+6p_z$ antibonding orbital forms a sharp resonance, which, according to a model calculation, decreases in energy as $R_{\text{Cu-Cs}}$ increases (*13*). This electronic change in response to the nuclear motion is recorded by time-resolved two-photon photoemission (2PP) (*6, 9*). This pump-probe method measures 2PP excited by a pair of identical laser pulses with a

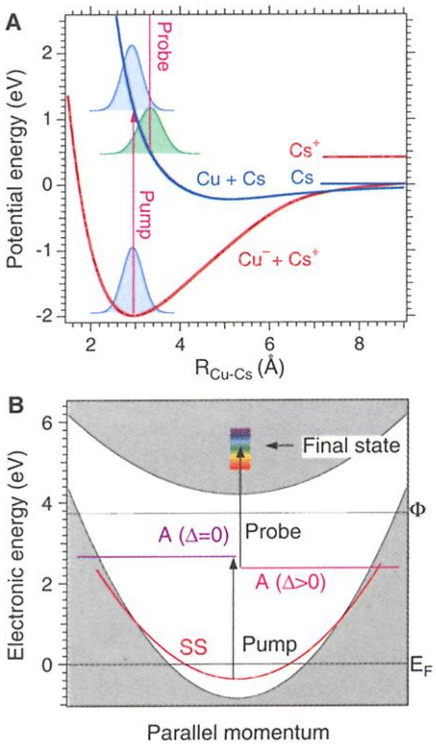

Fig. 1. (**A**) Schematic PESs are constructed following the procedure in (*9*). The energy of adsorption of Cs^+ (1.9 eV) and equilibrium $R_{\text{Cu-Cs}}$ (2.97 Å) for the ground state (red) are from thermal desorption (*9*) and theory (*13*). The excited state (blue) is constructed with a van der Waals potential for the Cs atoms and a repulsive term that gives the correct excitation energy (*5*). The asymptotic energies of the Cs^+ and Cs products are indicated by red and blue horizontal lines, respectively (*9*). The pump pulse projects the ground-state wave packet (represented by a blue gaussian distribution) onto the excited state, "turning on" the repulsive forces. The evolving wave packet (green distribution) is detected by the delayed probe pulse–induced photoemission from the $6s+6p_z$ antibonding state. (**B**) Band structure for Cu(111), indicating the band gap (unshaded area) and the 2PP excitation scheme. The color gradient for the final state conveys different energies for observation of the dynamics of *A*. The energy of *A* decreases approximately quadratically with the delay Δ.

Advanced Research Laboratory, Hitachi, Ltd., Hatoyama, Saitama 350-0395, Japan.

*To whom correspondence should be addressed. E-mail: petek@pitt.edu

†Present address: Department of Chemical Physics, Fritz-Haber Institute, Faradayweg 4-6, D-14195 Berlin, Germany.

‡Permanent address: Department of Physics and Astronomy, University of Pittsburgh, Pittsburgh, PA 15260, USA.

well-defined mutual delay Δ. The energy-resolved photoelectron current, which carries the information on the unoccupied electronic states, is recorded for normal emission (*15*).

The band structure of Cu (Fig. 1B) has crucial properties for the observation of Cs atom dynamics. A band gap between −0.85 and 4.1 eV (relative to the Fermi energy E_F) excludes electron propagation within the metal normal to the surface [(111) direction] and supports both an intrinsic occupied surface state (*SS*) at −0.39 eV (*6*) and an unoccupied Cs antibonding state (*A*) at ~3.1 eV (in the limit of zero CS coverage). Both surface states have restricted electronic relaxation channels, because the band gap confines their wave functions to the metal–vacuum interface (*9, 13*). The *SS* → *A* excitation energy is tuned into resonance with 3.08-eV light by varying the Cs coverage, which mainly affects the energy of *A* (E_A) (*16*).

A series of two-pulse correlation (2PC) scans (Fig. 2A) provide information on the dynamics of the antibonding state. These pump-probe measurements are performed by scanning Δ for ±240 fs while monitoring the 2PP signal for selected photoelectron energies. For near-resonant *SS* → *A* excitation, the 2PCs consist of a fast ≤15-fs decay of the coherent polarization (*9, 17*) and a slower, strongly energy-dependent, nonexponential decay corresponding to the antibonding state population dynamics. Simple electronic quenching of Cs should follow an exponential decay law. The observed nonexponential kinetics must therefore have an inherently different origin, such as a change in the surface electronic structure due to the dissociative motion of Cs atoms.

To test this hypothesis, the 2PC scans were simulated by an optical Bloch equation (OBE) formalism which describes the optical coupling of multiple electronic states (*6, 17*). The model for excitation of 2PP in Fig. 1B consists of *SS*, *A*, and a final state that is selected by the analyzer. The polarization and population decay times for *A* are set in the simulation to 15 and 50 fs (*9*), respectively. Furthermore, the energy $E_A(\Delta)$ is decreased by 0.12 eV over 100 fs to account for the dissociative motion. This change has a quadratic dependence if both $E_A(R_{\text{Cu-Cs}})$ and the dissociative PES can be approximated by linear functions. The OBE simulation reproduces the experiment remarkably well (Fig. 2B).

A more graphic demonstration of the wave packet dynamics is given by 2PP difference spectra (Fig. 3), in which the pump creates the wave packet and the probe tests its evolution. The difference spectra are constructed by recording 2PP spectra with well-defined delays between pump and probe pulses and then subtracting a reference background for a long (240 fs) delay to remove the 2PP component excited by each separate pulse. Consistent with the dissociative motion of Cs atoms, the electron density corresponding to *A* both changes in width and decreases in energy over time.

Plots of $E_A(\Delta)$ and its transformation into $R_{\text{Cu-Cs}}(\Delta)$ in Fig. 4 provide direct information on the mechanical forces acting on the Cs atom, and therefore, the excited-state potential energy surface in the vicinity of the ground-state equilibrium $R_{\text{Cu-Cs}}$. The nuclear wave packet motion can be deduced from

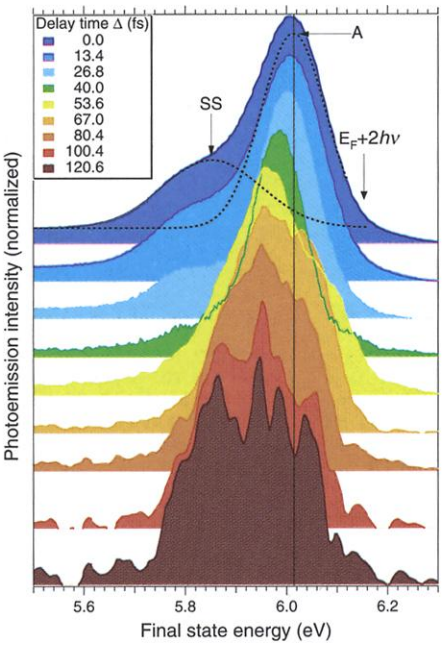

Fig. 3. The 2PP difference spectra give information on the dynamic surface electronic structure. The 2PP signal corresponds to one-photon absorption from both the pump and probe pulse, with the delay Δ set to an integral number of optical cycles. Dashed lines and solid vertical line indicate the gaussian peak deconvolution of *SS* and *A*, and energy of *A* at Δ = 0 fs, respectively. Interference effects in the wave packet creation and propagation might contribute to the complex changes in the line shapes. For Δ > 50 fs, $E_A(\Delta)$ is set to the peak of a gaussian line shape fitted to the lowest-energy edge of the antibonding state spectrum.

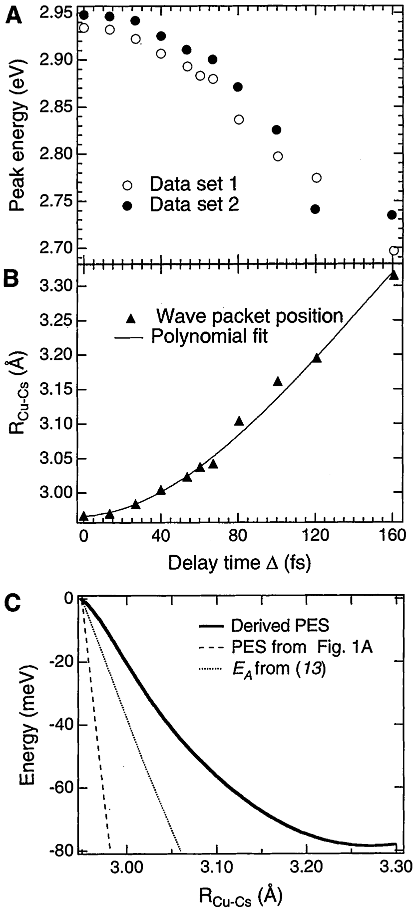

Fig. 4. (**A**) $E_A(\Delta)$ from two independent experiments for $\Theta_{\text{Cs}} \sim 0.09$ ML. (**B**) The wave packet position $R_{\text{Cu-Cs}}(\Delta)$ and its polynomial fit. (**C**) Dashed and solid lines, respectively, represent the predicted (Fig. 1A) and derived excited state PES near the ground-state equilibrium geometry, and the dotted line represents the calculated antibonding state energy dependence on $R_{\text{Cu-Cs}}$ (*15*).

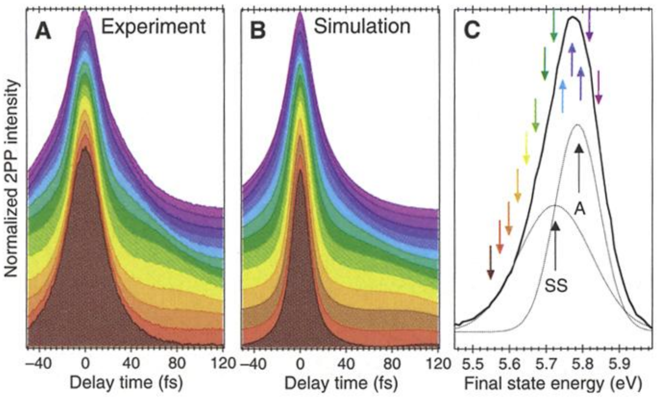

Fig. 2. (**A**) A series of 2PC scans taken for different observation energies for near-resonant *SS* → *A* excitation. The corresponding color arrow in the 2PP spectrum (panel C) indicates the energy for each 2PC measurement. (**B**) Simulation of 2PCs by OBE with the excitation scheme in Fig. 1B. The main difference between experiment (A) and theory (B) are the widths of the fast-decay component arising from omission of the bulk continuum states from the model, which dominate the 2PP signal below the *SS* → *A* resonance. In addition, a possible decrease in the ionization cross section and change in lifetime of *A* due to the increase in $R_{\text{Cu-Cs}}$ may affect the 2PC scans (*13*). (**C**) The 2PP spectrum for near-resonant *SS* → *A* excitation.

Fig. 3 by inverting the time-dependent orbital energy $E_A(\Delta)$ into time-dependent position $R_{\text{Cu-Cs}}(\Delta)$ via the calculated dependence of the $6s+6p_z$ orbital energy on $R_{\text{Cu-Cs}}$ (*13*). A fit of $R_{\text{Cu-Cs}}(\Delta)$ to a fourth-order polynomial gives a continuous function $R(\Delta)$, which is differentiated to obtain the acceleration of Cs atoms $a=\partial^2R(\Delta)/\partial\Delta^2$. The force acting on Cs atoms, $F = ma$, is then integrated, $U = -\int FdR$, to derive the experimental PES (Fig. 4C). This classical model explains the unusual nonexponential decay of the antibonding state in terms of a stretching of the Cu–Cs bond by ~0.35 Å within 160 fs of the excitation (*18*).

Although the Cu–Cs bond elongation is considerable, the most probable outcome of the photoexcitation is electronic relaxation back to the ground state. The desorption yield can be estimated from an increase in the work function Φ due to a photoinduced decrease of the Cs coverage (*19*), which gives an upper limit for the photodesorption cross section $\sigma_{\text{Cs/Cu}}$ of 2.4×10^{-23} cm^2. By contrast, the cross section for desorption of K from graphite $\sigma_{\text{K/C}}$ is 2×10^{-20} cm^2 (*5*). These two chemisorption systems probably have similar excitation probabilities and excited state lifetimes (*5*), and such a large difference in the cross sections must therefore arise from both different PES topologies and nuclear masses. This conclusion is consistent with the experimentally derived PES, which is much less repulsive at the point of excitation for Cs/Cu(111) than for K/C. Furthermore, the present one-dimensional model does not consider the recoil motion of substrate Cu atoms, which will lead to a significant transfer of energy to bulk phonons. These differences imply that photoexcitation imparts less velocity to Cs than to K, making its chance of escape much smaller for a comparable lifetime.

A possible extension of these results is to apply the photoinduced displacement of alkali atoms in an ultrafast atomic switch. Eigler demonstrated a switch based on reversible transfer of Xe atoms between a Ni(110) surface and a scanning tunneling microscope (STM) tip (*20*). A plausible mechanism for the transfer is vibrational heating through multiple cycles of excitation and relaxation involving electron scattering through the unoccupied 6s orbital of Xe (*21*). Because of the limited excitation rate and inelastic scattering probability, however, the Eigler switch is inherently slow (on the order of a nanosecond). Femtosecond-length laser excitation could also actuate alkali atom transfer in a surface-STM junction. The chemisorption strength of Cs and excited-state distension are adequate to induce transfer in a single photoexcitation step. With a <200-fs transfer time, such a device could be many orders of magnitude faster and more efficient than the Eigler switch.

The possibility of resolving the nuclear motion of atoms and molecules on surfaces at femtosecond and angstrom scales through time-resolved photoemission spectroscopy has been demonstrated. Recent studies of other alkali atom adsorbates and noble metal substrates suggest that Cs/Cu(111) is not unique (*16*). Systematic studies of other systems will lead to a more complete understanding of the principles involved in the electronic relaxation, desorption, and atomic manipulation of metal surfaces.

References and Notes

1. H.-L. Dai and W. Ho, Eds., *Laser Spectroscopy and Photochemistry on Metal Surfaces*, vol. 5 (World Scientific, Singapore, 1995).
2. D. Menzel and R. Gomer, *J. Chem. Phys.* **41**, 3311 (1964).
3. L. Bartels *et al.*, *Phys. Rev. Lett.* **80**, 2004 (1998).
4. F. M. Zimmermann and W. Ho, *Surf. Sci. Rep.* **22**, 127 (1995).
5. B. Hellsing, D. V. Chakarov, L. Österlund, V. P. Zhadanov, B. Kasemo, *J. Chem. Phys.* **106**, 982 (1996).
6. H. Petek and S. Ogawa, *Prog. Surf. Sci.* **56**, 239 (1997).
7. U. Höfer *et al.*, *Science* **277**, 1480 (1997).
8. N.-H. Ge *et al.*, *Science* **279**, 202 (1998).
9. S. Ogawa, H. Nagano, H. Petek, *Phys. Rev. Lett.* **82**, 1931 (1999).
10. R. D. Diehl and R. McGrath, *J. Phys. Condens. Matter* **9**, 951 (1997).
11. A. M. Bradshaw, H. P. Bonzel, G. Ertl, *Physics and Chemistry of Alkali Metal Adsorption* (Elsevier, Amsterdam, 1989).
12. J. P. Muscat and D. M. Newns, *Surf. Sci.* **84**, 262 (1979).
13. A. G. Borisov, A. K. Kazansky, J. P. Gauyacq, *Surf. Sci.* **430**, 165 (1999).
14. H. Ishida and A. Liebsch, *Phys. Rev. B* **45**, 6171 (1992).
15. The excitation source is a frequency-doubled (3.08 eV) Ti:sapphire laser producing an 80-MHz train of 16-fs pulses with <0.5 nJ energy. Delay between the pulse-pair is set within 5×10^{-17} s (1/25 of a cycle of 400-nm light) by a Mach-Zehnder interferometer. A single-crystal Cu(111) surface is covered under ultrahigh vacuum by 0.08 to 0.10 monolayer (ML) of Cs atoms (coverage ΘCs of 1.8×10^{15} atoms/cm^2 corresponds to 1 ML), and cooled to 33 K.
16. H. Petek, M. J. Weida, H. Nagano, S. Ogawa, *Surf. Sci.* **451**, 22 (2000).
17. S. Ogawa, H. Nagano, H. Petek, *Surf. Sci.* **427/428**, 34 (1999).
18. Alternative explanations involving inhomogeneous effects leading to site- or energy-dependent antibonding state lifetimes are excluded for the following reasons: (i) *A* is homogeneously broadened, as reported in (*11*); (ii) although an inhomogeneous sample can result in multiexponential decay, it is difficult to construct a mechanism that could explain the observed nonexponential decay; (iii) the lifetime of *A* is independent of energy between 2.4 and 3.2 eV at 300 K [M. Bower, S. Pawlik, M. Aeschlimann, *Phys. Rev. B* **60**, 5016 (1999)]; and (iv) a quadratic dependence of $E_A(\Delta)$ would be highly coincidental.
19. S. Ogawa, M. J. Weida, H. Nagano, H. Petek, unpublished data.
20. D. M. Eigler, C. P. Lutz, W. E. Rudge, *Nature* **352**, 600 (1991).
21. S. Gao, M. Persson, B. I. Lundqvist, *Solid State Commun.* **84**, 271 (1992).

22. We acknowledge N. Moriya, S. Matsunami, and S. Saito for technical support and NEDO for partial funding for this project through the International Joint Research Grant. M.J.W. thanks NSF and the Center for Global Partnership for support (NSF grant INT-9819100).

17 January 2000; accepted 4 April 2000

Electron-Induced Inversion of Helical Chirality in Copper Complexes of *N*,*N*-Dialkylmethionines

Steffen Zahn and James W. Canary*

Stereodynamic complexes of copper were found to undergo inversion of a helical chiral element upon oxidation or reduction. The amino acid methionine was derivatized by the attachment of two chromophores to the nitrogen atom. The resultant ligands formed stable complexes with Cu^{I} and Cu^{II} salts. For a derivative of a given absolute chirality, the complexes afford nearly mirror image circular dichroism spectra. The spectral changes originate from reorientation of the nitrogen-attached chromophores due to a conformation interconversion driven by the exchange of a carboxylate for a sulfide ligand. The electrically induced chirality inversion coupled with strong interactions with polarized light is unique and may lead to novel chiral molecular devices.

Manipulation of the handedness of molecular shape is an uncommon but potentially very useful phenomenon. Inversion of the helical chirality formed by aromatic substituents has been achieved by photochemical isomerization of aryl-substituted alkenes (*1–3*) or by photochemical electrocyclic reactions (*3*). For systems that also show photochroism, reversible inversion of helical chirality may be achieved by monochromatic light. These studies have generated interest in molecular electronics applications, although one problem that has been encountered is destructive readout (*4*). Here, we

---

Department of Chemistry, New York University, New York, NY 10003, USA.

*To whom correspondence should be addressed. E-mail: james.canary@nyu.edu